



HAL
open science

KarstMod User Guide - version 2.2

Naomi Mazzilli, Dominique Bertin

► **To cite this version:**

| Naomi Mazzilli, Dominique Bertin. KarstMod User Guide - version 2.2. 2019. hal-01832693v1

HAL Id: hal-01832693

<https://hal.science/hal-01832693v1>

Preprint submitted on 18 Mar 2019 (v1), last revised 28 Feb 2023 (v2)

HAL is a multi-disciplinary open access archive for the deposit and dissemination of scientific research documents, whether they are published or not. The documents may come from teaching and research institutions in France or abroad, or from public or private research centers.

L'archive ouverte pluridisciplinaire **HAL**, est destinée au dépôt et à la diffusion de documents scientifiques de niveau recherche, publiés ou non, émanant des établissements d'enseignement et de recherche français ou étrangers, des laboratoires publics ou privés.



KarstMod

User Guide

version 2.2
2018/07

Mazzilli N., Bertin D.



About KarstMod

KarstMod is a collaborative project developed by the French SNO Karst (<http://www.sokarst.org/>). It provides an adjustable modeling platform for both the simulation of spring discharge at karst outlets and the analysis of the hydrodynamics of the compartments considered in the model. This platform is developed within the framework of the KARST observatory network initiative from the INSU/CNRS, which aims to strengthen knowledge-sharing and promote cross-disciplinary research on karst systems at the national scale.

KarstMod is a free software that comes with absolutely no warranty. You are welcome to redistribute it. Please refer to the license menu for distribution details.

Contact: karstmod@services.cnrs.fr

Please cite us as : Mazzilli N., Guinot V., Jourde H., Lecoq N., Labat D., Arfib B., Baudement C., Danquigny C., Dal Soglio L. & Bertin D. (2017). KarstMod: A modelling platform for rainfall - discharge analysis and modelling dedicated to karst systems. Environmental Modelling & Software 2017 [doi:10.1016/j.envsoft.2017.03.015](https://doi.org/10.1016/j.envsoft.2017.03.015)

Contents

1	KarstMod overview	3
2	Model structure and equations	3
2.1	Structure	3
2.2	Equations	3
2.2.1	Internal Fluxes for classical compartment configuration	3
2.2.2	Internal Fluxes for infinite characteristic time configuration	5
2.2.3	Balance equations	6
2.2.4	Discharge at the outlet	6
2.3	Equivalent piezometric level	6
2.4	Model solution	7
3	Model calibration	7
3.1	Warm-up, calibration and validation periods	7
3.2	Calibration procedure	7
3.2.1	Calibration variable	7
3.2.2	Performance criteria	7
3.2.3	Objective function	8
4	Model outputs	8
4.1	Optimal simulation analysis	8
4.2	Equifinality analysis	8
5	Getting started	10
5.1	Requirements	10
5.2	Interface	10
5.2.1	Model Structure	10
5.2.2	Data	10
5.2.3	Filling gaps in discharge or piezometric data	11
5.2.4	Model Parameters	11
5.2.5	Run parameters	11
5.2.6	Calibration results	12
5.2.7	Command bar	12
5.2.8	Graphics	12
5.3	File format	13
5.3.1	Input data	13
5.3.2	Output files	14
6	Example	14
A	Model solution	18
A.1	Analytical solutions (linear cases)	18
A.1.1	Analytical solution - Linear rainfall-discharge case with no inter-compartment coupling	18
A.1.2	Analytical solution for rainfall-discharge relationship with inter-compartment coupling	18
A.2	Linearized formulations	20
	List of Notations	21
	References	22

1 KarstMod overview

KarstMod is an adjustable modelling platform for simulating the rainfall-discharge relationship of karst springs at a daily or hourly time step and for analyzing the hydrodynamics of the compartments considered in the model. This modular, user-friendly modelling environment can be used for educational, research and operational purposes. It can reproduce the structure of most conceptual global models of karst systems found in the literature. The modularity of the platform makes it possible to compare different hydrosystems within a same methodological approach. To promote good modelling practices, the platform provides a variety of graphs and tools that help gain understanding and insight into the behaviour of the model, and also help the user detect possible flaws in structure and parameterization.

In the first step, the user defines the model structure and fluxes using the graphical interface. Global models are based on physically sound structures and equations. The user may thus use his understanding of the primary processes involved to define the model. However, we recommend a gradual complexification approach, with careful assessment of the influence of the selected compartment and fluxes on resulting model behaviour and equifinality. User-defined values of rainfall, evapotranspiration and pumping in the compartments are specified in the next step. The user also defines the performance measure and the warm-up, calibration and validation periods.

The model may run based on user-specified parameter values (“run mode”) or in an automatic calibration mode. Most model outputs are available in both run and calibration modes. Calibration mode provides a systematic exploration of the parameters space. The outcomes of this exploration are the selection of the optimal parameter set for the selected performance measure, and a set of graphs that allow a first grasp of equifinality issues. Run mode may be especially useful for educational purposes.

2 Model structure and equations

2.1 Structure

In its most complete form, the platform offers 4 compartments organized as a two-level structure: (i) compartment E (higher level), (ii) compartments L, M and C (lower level). In its most simplified form, the structure is reduced to compartment E only, which cannot be deactivated.

Two configurations are available for each compartment : (i) classical configuration, (ii) infinite characteristic time configuration. These two configurations are detailed in Sections 2.2.1 and 2.2.2. In the classical configuration the user may activate a number of transfer law with finite characteristic transfer time. In the infinite characteristic time configuration, a transfer law with infinite characteristic time is applied. Figure 1 provides an overview of the available configurations for each compartment.

2.2 Equations

2.2.1 Internal Fluxes for classical compartment configuration

Q_{AB} discharge - water level functions ($Q_{EM}, Q_{EC}, Q_{ES}, Q_{LS}, Q_{MS}, Q_{CS}$) The general notation Q_{AB} indicates that the flux is taken from compartment A to compartment B.

Q_{AB} is defined by

$$Q_{AB} = k_{AB} \left(\frac{A}{L_{ref}} \right)^{\alpha_{AB}} \quad \text{if } A > 0 \quad (1a)$$

$$Q_{AB} = 0 \quad \text{otherwise} \quad (1b)$$

where A is the water level in compartment A and k_{AB} is the specific discharge coefficient [L/T] for the discharge law from compartment A to compartment B, L_{ref} [L] is a unit length and α_{AB} [-] is a positive exponent.

Threshold loss function (Q_{loss}) The Q_{loss} function is defined as follows:

$$Q_{loss} = k_{loss} \left(\frac{E - E_{loss}}{L_{ref}} \right)^{\alpha_{loss}} \quad \text{if } E > E_{loss} \quad (2a)$$

$$Q_{loss} = 0 \quad \text{otherwise} \quad (2b)$$

where k_{loss} [L/T] is the specific discharge coefficient for the Q_{loss} function, E_{loss} [L] is the threshold for the activation of the Q_{loss} function, and α_{loss} [-] is a positive exponent.

Hysteretic discharge functions ($Q_{hy}, Q_{hyEC}, Q_{hyES}$) Hysteretic discharge - water level function from compartment E to compartment C and / or to the outlet S is defined as follows:

$$Q_{hy} = \varepsilon_{HY} \times k_{hy} \left(\frac{E - E_{hy}}{L_{ref}} \right)^{\alpha_{hy}} \quad (3a)$$

$$Q_{hyEC} = x_{hy} \times Q_{hy} \quad (3b)$$

$$Q_{hyES} = (1 - x_{hy}) \times Q_{hy} \quad (3c)$$

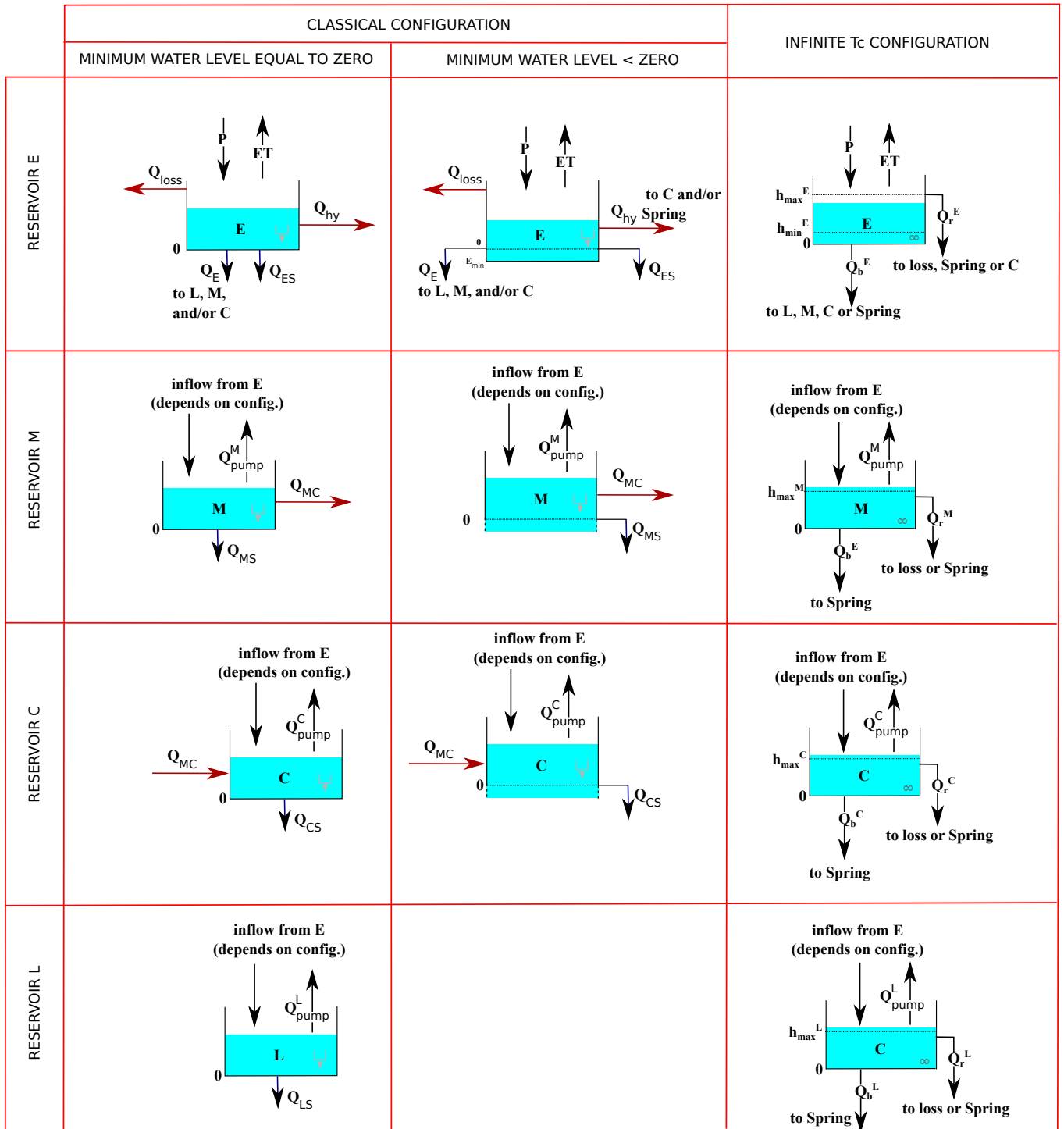


Figure 1: Structure of the modular platform : Possible configurations for each compartment.

In the classical configuration, default minimum water level in compartments L, M and C is zero. In compartment E, the minimum water level can be either zero or less (soil available water content configuration). In compartments M and C, the minimum water level can be either zero or less (bottomless configuration).

For compartment L and in infinite characteristic time configuration, minimum water level is zero.

where k_{hy} is the specific discharge coefficient [L/T], α_{hy} is a positive exponent [-], $x_{hy} \in [0, 1]$ [-] and ε_{hy} [-] is an indicator of the activation of the hysteretic discharge. ε_{hy} is switched to 1 if E rises above $E_{hy} + \Delta E_{hy}$ and it is switched to 0 if E falls below E_{hy}

$$\left. \begin{array}{l} \varepsilon_{HY} = 0 \\ E = E_{hy} + \Delta E_{hy} \end{array} \right\} \Rightarrow \varepsilon_{HY} = 1 \quad (4a)$$

$$\left. \begin{array}{l} \varepsilon_{HY} = 1 \\ E = E_{hy} \end{array} \right\} \Rightarrow \varepsilon_{HY} = 0 \quad (4b)$$

Warning When the exponent coefficient α is set to 1, the associated discharge function becomes linear.

Warning When ΔE_{hy} is set to zero, the hysteretic Q_{hy} function simplifies to a threshold discharge function similar to Q_{loss} .

Exchange function (Q_{MC}) The Q_{MC} function is defined as follows:

$$Q_{MC} = k_{MC} \times \text{sgn}(M - C) \times \left| \frac{M - C}{L_{ref}} \right|^{\alpha_{MC}} \quad (5)$$

where k_{MC} [L/T] is the specific discharge coefficient, and α_{MC} [-] is a positive exponent.

Warning Q_{MC} is defined as the algebraic flow from compartment M to compartment C. Negative Q_{MC} values mean that the current direction of flow is from C to M.

Warning When the inter-compartment flux Q_{MC} is activated, the M and C compartments must be either both bottomless, or both with bottom. Q_{MC} activation also requires the classical configuration to be selected for both M and C.

2.2.2 Internal Fluxes for infinite characteristic time configuration

A detailed description of the infinite characteristic time transfer function is given in [5]. The purpose of this transfer function is to account for multiple transfer time scales in hydrosystems using a single compartment, thus preserving model structure simplicity. It may be used to account for dual flow behaviours, where sharp discharge peaks are associated with slowly decreasing base discharge signal. In what follows, the compartment under consideration is denoted by A hereafter. R is the inflow rate to A. R might e.g. be equal to $P - ET$ for compartment E, $Q_{EL} - Q_{pumpL}$ for compartment L, etc. The unit response $\omega(t)$ of a compartment A with an infinite characteristic time is defined as follows :

$$\omega(t) = \frac{\alpha_A \times \tau_A^{\alpha_A}}{(\tau_A + t)^{\alpha_A + 1}} \quad (6)$$

where $\alpha_A \in (0, 1)$ is an exponent and τ_A is a time scale. Note that $\alpha_A \geq 1$ would yield a finite characteristic time scale. The outflowing discharge Q_{bA} from compartment A is related to the inflow R by the convolution product :

$$Q_{bA} = R \circledast \omega(t) \quad (7)$$

For the sake of computational efficiency, the convolution kernel is approximated with a set of local operators run in parallel. This amounts to partitioning the compartment A into n sub-compartments with linear discharge laws, all running in parallel. The water level $A(t)$ in compartment A is equal to the weighted sum of the water levels $A_i(t)$ in the n sub-compartments, and the outflowing discharge rate Q_{bA} from compartment A is given by the weighted sum of the specific outflow rates Q_{bAi} from the n sub-compartments:

$$A(t) = \sum_{i=1}^n \theta_i A_i(t) \quad (8a)$$

$$Q_{bA}(t) = \sum_{i=1}^n \theta_i Q_{bAi}(t) \quad (8b)$$

$$\sum_{i=1}^n \theta_i = 1 \quad (8c)$$

An upper threshold $h_{\max A}$ is set for the depth in the sub-compartments. When the water level A_i becomes larger than $h_{\max A}$, the i th sub-compartment is bypassed and the corresponding overflow Q_{rAi} is routed directly to either the spring, losses or compartment C (this latter being only available for an infinite characteristic time configuration on compartment E). Note that such rapid overflow may occur even though the average water level $A(t)$ is below the upper threshold

$h_{\max A}$. Indeed, some sub-compartments may pass the $h_{\max A}$ threshold while the weighted sum $A(t)$ stays below $h_{\max A}$. The total overflow Q_{rA} is given by the weighted sum of the specific outflow rates Q_{rAi} from the n sub-compartments:

$$Q_{rA}(t) = \sum_{i=1}^n \theta_i Q_{rAi}(t) \quad (9)$$

When the infinite characteristic time configuration is applied to compartment E, an additional threshold $h_{\min E}$ may be set for the depth in the sub-compartments (soil available water content configuration). In this case PET is subtracted from the compartment only if the average depth E is above threshold $h_{\min E}$. For $E < h_{\min E}$, water is assumed to be unavailable for plant uptake and/or evaporation, but note that infiltration through flows Q_{bE} , Q_{rE} may still occur.

2.2.3 Balance equations

The model has 4 balance equations. These balance equations are detailed hereafter in their complete form. Please note that all fluxes can not be activated together (for example, classical and infinite Tc configurations are mutually exclusive). Also note that some of these fluxes may be directed to different compartment based on user selection : for example, rapid overflow discharge from compartment E in infinite Tc configuration Q_r^E may be directed to either compartment C, to the spring, or to losses.

$$\frac{dE}{dt} = P - ET - Q_{loss} - Q_{EL} - Q_{EM} - Q_{ES} - Q_{EC} - Q_{hy} - Q_{bE} - Q_{rE} \quad \text{if } E \geq 0 \quad (10a)$$

$$\frac{dE}{dt} = P - ET \quad \text{if } E_{min} < E < 0 \quad (10b)$$

$$\frac{dL}{dt} = Q_{EL} + Q_{bE} - Q_{LS} - Q_{pump}^L - Q_{bL} - Q_{rL} \quad (10c)$$

$$\frac{dM}{dt} = Q_{EM} + Q_b^E - Q_{MC} - Q_{MS} - Q_{pump}^M - Q_{bM} - Q_{rM} \quad (10d)$$

$$\frac{dC}{dt} = Q_{EC} + Q_{bE} + Q_{rE} + Q_{hyEC} + Q_{MC} - Q_{CS} - Q_{pump}^C - Q_{bC} - Q_{rC} \quad (10e)$$

where:

- E , L , M and C [L] are water levels in compartments E, L, M and C respectively,
- E_{min} [L] is the minimum water level in compartment E,
- P [L/T] is the precipitation rate,
- ET [L/T] is the evapotranspiration rate,
- Q_{pump}^L , Q_{pump}^M and Q_{pump}^C [L/T] are the discharge rates abstracted from compartment L, M and C respectively, per unit surface area,
- Q_{loss} , Q_{EM} , Q_{ES} , Q_{EC} , Q_{hy} , Q_{hyEC} , Q_{hyES} , Q_{LS} , Q_{MS} , Q_{CS} , Q_{MC} [L/T] are internal discharge rates per unit surface area, for classical configuration of the E, L, M, C compartments,
- Q_{bE} , Q_{rE} , Q_{bL} , Q_{rL} , Q_{bM} , Q_{rM} , Q_{bC} , Q_{rC} , [L/T] are internal discharge rates per unit surface area, for infinite Tc configuration of the E, L, M, C compartments.

2.2.4 Discharge at the outlet

Discharge at outlet Q_S depends on the recharge area, on the activated fluxes to the spring and on abstraction rate at the outlet. It is given by the following equation:

$$Q_S = R_A \times (Q_{ES} + Q_{LS} + Q_{MS} + Q_{CS} + Q_{hyES} + Q_{rE} + Q_{rLS} + Q_{rMS} + Q_{rCS} + Q_{bLS} + Q_{bMS} + Q_{bCS} - Q_{pump}^S) \quad (11)$$

where R_A [L²] is the catchment recharge area and Q_{pump}^S [L/T] is the discharge rate abstracted at the outlet per unit surface area.

2.3 Equivalent piezometric level

An equivalent piezometric level Z can be derived from the water level in compartment A (where A stands for either E, L, M, or C).

$$Z = Z_0 + \frac{A}{w} \quad (12)$$

where Z_0 [L] is the elevation of the compartment overflow threshold and w [-] is the effective porosity.

2.4 Model solution

In compartments where all exponents are set equal to 1, we use the analytical solution of the differential model equations. Non-linear formulations (exponent different from 1) are solved using a second-order Runge-Kutta scheme of the linearized formulation (see Appendix A).

3 Model calibration

3.1 Warm-up, calibration and validation periods

Warm-up, calibration and validation periods are defined as follows:

- The warm-up period corresponds to the time interval after which the initialization bias is deemed negligible. Simulation results from the warm-up period are not considered in the calibration. Therefore, discharge measurements at the outlet are not required during this period.
- The calibration period corresponds to the time interval over which the calibration is performed, that is, model performance during this time period is used to select the optimal parameter set.
- The validation period corresponds to the time interval over which the model performance is evaluated, but not used for calibration purpose.

Warning Warm-up, calibration and validation periods are entirely controlled by the user (see section 5) but :

- If the warm-up period is too short, calibration results may depend on the initial water level
- The calibration period should cover a large range of hydrological conditions

Remark The model provides the possibility of calibrating the initial water level in the activated compartments. Also note that discontinuous calibration and validation periods are allowed. See section 5 for details.

3.2 Calibration procedure

The model is calibrated using a quasi Monte-Carlo procedure, with a Sobol sequence sampling of the parameter space [17]. The procedure is stopped when either n_{max} parameter sets satisfying a minimum value of the objective function $WOBJ > WOBJ_{min}$ are collected, or when the elapsed simulation time reaches the maximum duration t_{max} specified by the user. Both $WOBJ_{min}$ and t_{max} are user-specified, see 5.2.5.

3.2.1 Calibration variable

Both the simulated discharge at the outlet and the equivalent piezometric water level (if defined) can be used as calibration variables.

3.2.2 Performance criteria

The performance criteria proposed in KarstMod are the Nash-Sutcliffe efficiency coefficient NSE [13], the Volumetric Efficiency [8], the modified Balance Error BE [14] and the Kling Gupta Efficiency KGE [7], defined as follows :

$$NSE = 1 - \frac{\sum (U_S - U_{obs})^2}{\sum (U_{obs} - \bar{U}_{obs})^2} \quad (13a)$$

$$VE = 1 - \frac{\sum |U_S - U_{obs}|}{\sum U_{obs}} \quad (13b)$$

$$BE = 1 - \left| \frac{\sum U_S - \sum U_{obs}}{\sum U_{obs}} \right| \quad (13c)$$

$$KGE = 1 - \sqrt{(r - 1)^2 + (\alpha - 1)^2 + (\beta - 1)^2} \quad (13d)$$

where U stands for either the discharge or the equivalent piezometric level, r is the Pearson correlation coefficient between the simulated and observed flow, β is the ratio between the mean simulated and mean observed flow, α is the ratio between the simulated and observed flow variance. The user may apply the performance criteria to either the full range of the variable or to values above or below discharge thresholds.

These four criteria can range from $-\infty$ to 1. Performance criteria of 1 for NSE, VE or KGE corresponds to a perfect match between model and observations. As regards the NSE, an efficiency of 0 indicates that the model performs equally to the mean of the observed data, whereas efficiencies less than zero occur when the observed mean is a better predictor than the model.

On the contrary, a constant model equal to the mean of the observed data yields a BE value of 1. As a consequence, a Balance Error of 1 means that the total flow volume discharged at the outlet is equal to that observed. The BE criteria is therefore used either as a constraint in a single objective optimization process or as an objective function in a multiple objective calibration exercise [4].

Warning The NSE does not measure model quality in absolute terms, but proposes a quantification in relative terms of how much better or worse the model performs in comparison to the benchmark observed mean [12]. Therefore, NSE should be considered carefully when comparing model performance over a variety of hydrological regimes.

3.2.3 Objective function

KarstMod allows either single or multi-objective calibration approaches. The objective function WOBJ used in the calibration procedure is either one of the performance criteria defined in Section 3.2.2 or an aggregated objective function defined by the user as the weighted sum of two of the performance criteria defined in Section 3.2.2. The multi-objective problem is thus reduced to a scalarized one.

4 Model outputs

4.1 Optimal simulation analysis

The optimal parameter set is defined as the parameter set of the Sobol sequence sampling that yields the best model performance over the calibration period, with respect to the objective function WOBJ. The optimal simulation is the simulation that results from a model run that uses the optimal parameter set. As regards the optimal simulation, the following graphs are available:

- rainfall, ET, simulated and observed discharge at the outlet as a function of time;
- rainfall, ET, internal discharge rates as a function of time;
- rainfall, ET, internal water levels (and observed and simulated piezometric levels, if available) as a function of time;
- cumulative volumes at the outlet as a function of time;
- simulated mass balance per time step;
- simulation error as a function of time;
- Q_S versus Q_{obs} plot.

These graphs make it possible to investigate the internal behaviour of the model and to detect possible drifts. The Q_S versus Q_{obs} plot highlights the variability of the simulation error during the simulation. The following analyses are also available as options:

- probability plots for the simulated (Q_S) and observed (Q_{obs}) discharges;
- auto-correlogram of Q_{obs} and Q_S ;
- cross-correlogram between P and Q_S ;
- cross-correlogram between P and Q_{obs} ;
- cross-correlogram between Q_{obs} and Q_S .

The discharge probability plots provide insights into processes that may influence the distribution law of discharge values, such as the existence of overflow springs, or the extra input or output of water coming from or going towards a neighbouring system [10, 11]. The simple and cross spectral analyses complete the study of the correlogram functions by providing information on the regulation time of the system (i.e. its inertia related to the nature of its storage) and on the frequency of the phenomena that produce flow variations at the spring [10].

4.2 Equifinality analysis

Overview Most environmental problems are ill-posed, i.e. encounter issues about the uniqueness, identifiability and stability of the problem solution [3]. As a consequence, many representations (model structures and parameter sets within a given model structure) of the modelled system may be considered acceptable [2]. In KarstMod, parametric equifinality can be investigated using the following tools:

- scatter plots of the values of the objective function (calibration period) against the values of the parameters X_i , for all parameter sets of the Sobol sequence that satisfy $W OBJ > W OBJ_{min}$. These plots provide a preliminary analysis of the distribution of the optimum values of each parameter.
- scatter plot of the values of the performance criteria used to define the aggregated objective function, for all the parameter sets of the Sobol sequence that satisfy $W OBJ > W OBJ_{min}$. These plots make it possible to investigate possible conflicts between the performance criteria (Pareto frontier) [6].
- variance-based, first-order S_i and total S_{T_i} sensitivity indexes for the model parameters X_i . These indexes aid in estimating the influence of parameters on model output, and thus in detecting over-parameterization.

Sensitivity indexes The sensitivity indexes are related to the decomposition of the variance of the calibration variable (here, discharge at the outlet) into terms that are due either to each parameter i taken singularly (first order indexes), or to interactions between parameters. The sensitivity index S_i for parameter X_i with respect to the simulated discharge Q_S is defined as the fraction V_i of the variance $V(Q_S)$ of the simulated discharge which is due solely to the parameter X_i : $S_i = \frac{V_i}{V(Q_S)}$. The total sensitivity index S_{Ti} measures the contribution of X_i to the output variance, including the interactions of X_i , of any order, with other input variables [15]. Both indexes are calculated using the Sobol procedure described in [16].

By default, the sensitivity indexes provided by KarstMod are obtained based on a $N = 1000 \times (n_{par} + 2)$ parameters set, where n_{par} is the number of parameters to be calibrated. Additional details also allow to check the convergence of the sensitivity indexes calculation:

- the sensitivity indexes are calculated and displayed for an increasing number of parameters sets (from $N = 1$ to $N = 1000 \times (n_{par} + 2)$) (sensitivity indexes graph),
- a 95% confidence interval on the sensitivity indexes is provided on the sensitivity indexes graph.

If the convergence is not reached, a user-defined number of parameter sets can be added to the sensitivity indexes calculation.

Parametric uncertainty of the simulation results KarstMod proposes to use the simulation results from all parameter sets yielding $WOBJ > WOBJ_{min}$ for the evaluation of the uncertainty on the simulation results. The approach is derived from the Regional Sensitivity Analysis (RSA) [9] and the Generalized Likelihood Uncertainty Estimation (GLUE) [1]. Instead of selecting a unique parameter set as the outcome of the calibration process, these methods consider that all parameter sets yielding satisfactory results over the calibration period (behavioural parameter sets) should be considered in the prediction process. The value of WOBJ over the calibration period is used as a likelihood measure for each behavioural parameter set. Based on this assumption, KarstMod proposes the following simulation results:

- $Q_S^{min}(t)$ and $Q_S^{max}(t)$ are defined as the minimal and maximal discharge values simulated at time step t from the behavioural parameter sets. They help determine the spread of the simulation results for the behavioural parameter sets.
- $Q_S^{prob}(t)$ is defined for a given time step (t) as the weighted sum of the simulated discharge $Q_S(t)$ with the objective function WOBJ, over all behavioural parameter sets: $Q_S^{prob}(t) = \frac{\sum_{i=1}^N WOBJ_{(i)} \times Q_{out(i)}(t)}{\sum_{i=1}^N WOBJ_{(i)}}$, where N is the number of behavioural parameter sets. $Q_S^{prob}(t)$ is an estimator of the most likely value of the simulated discharge, considering the user-defined objective function and the user-defined threshold value for the definition of the behavioural set.
- $Q_S^{0.05}(t)$ and $Q_S^{0.95}(t)$ are the 90% confidence interval limits for the simulated discharge at time t , computed over the behavioural parameter sets using the likelihood as a weighting factor.

5 Getting started

5.1 Requirements

KarstMod is Jar-packaged software. The minimum requirement for running KarstMod is the 64 bits version of JRE (Java Runtime Environment) 1.8 . The KarstMod.jar file can be executed by simply double-clicking the jar file. Open-JDK users should also install the open-jfx package.

5.2 Interface

The application window is divided into 7 areas (see Figure 2).

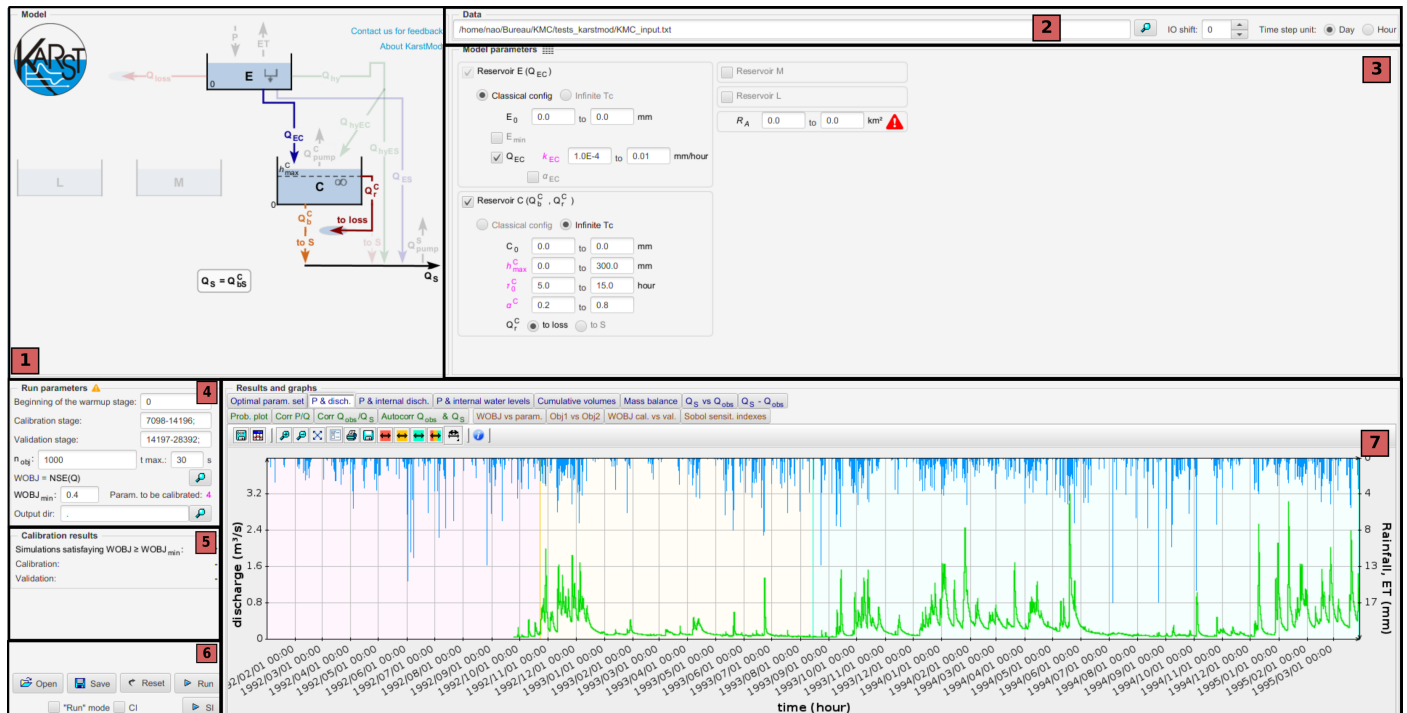


Figure 2: Interface areas: 1) Model structure, 2) Data, 3) Model parameters, 4) Run parameters, 5) Calibration results, 6) Command bar, 7) Graphs

5.2.1 Model Structure

The Model Structure area displays the model structure (see Figure 3). At the first opening of KarstMod, all compartments are deactivated except compartment E, and compartments configuration (either classical or infinite Tc) is undefined. The user must first select compartment type by clicking on the “?” symbol. Once compartment type is selected, the user proceeds to activation of selected transfer functions by clicking on the related arrows. When the user places the mouse over one element, its name appears in a pop-up window and the input block for these parameters is highlighted in blue (see 5.2.4). Inactive compartments and fluxes are grayed out. All elements can be activated or deactivated by pressing the space bar or by clicking on the element except compartment E which cannot be deactivated. When a compartment is deactivated, the related elements are also deactivated. When reactivated, the related elements are restored to their previous state. The formula located below is updated depending on the elements activated.

5.2.2 Data

This block makes it possible to:

- select the data file to use
- choose the time-lag (in number of time steps) between outputs and inputs (0 by default)
- choose the time-step unit, which represents the time step between two pieces of data in the file. The input time series must be suitable for the chosen time step. Changing the unit involves updating the units indicated in other blocks and graphs in the window.

In the event of gaps in the sequence of observed discharges and piezometric levels, the value “INTERP” or “NOINTERP” must be applied in the input file to indicate the absence of data over the time steps concerned (see input file format in 5.3.1).

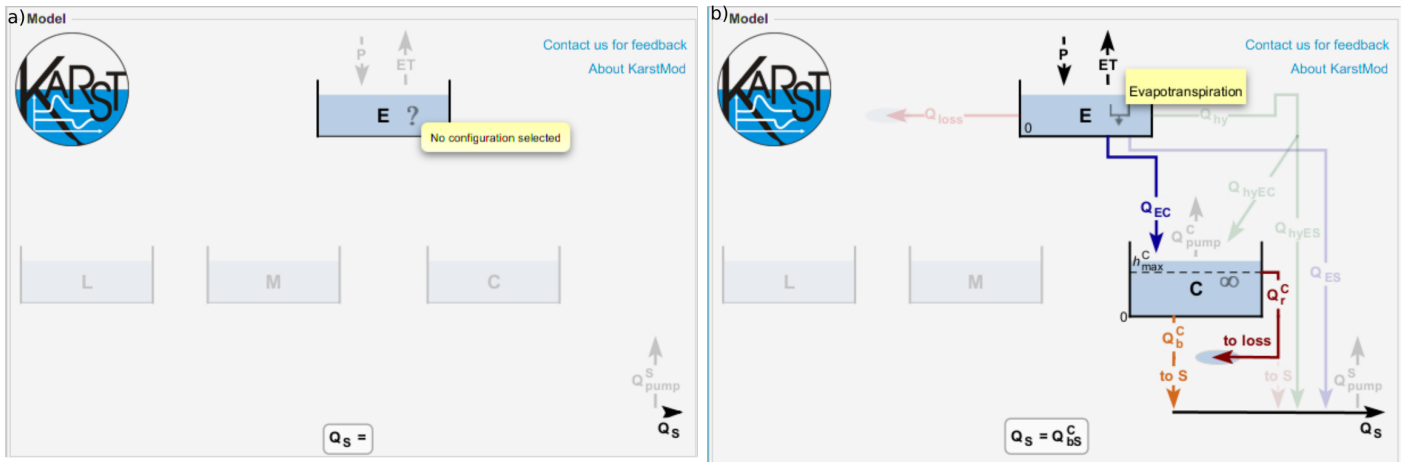


Figure 3: Model structure interface area: a) at software launching, compartment configuration is undefined, b) configuration example

5.2.3 Filling gaps in discharge or piezometric data

Gaps indicated with the “INTERP” value in the observed discharged or piezometric levels times series can be filled using a Lagrange polynomial interpolation. The interpolation utility pops up when the input data file is loaded. The order of the interpolation is defined by the user. The interpolation may be restricted to gaps shorter than a user-defined number of steps.

Gaps indicated with the “NOINTERP” value and gaps indicated with an “INTERP” value but with a length greater than the maximum gap interpolation length defined by the user are not filled.


5.2.4 Model Parameters

This block is for inputting the range of values of model parameters from activated elements. Note that activation / deactivation of most fluxes can only be performed in the “Model Structure” area. “Model Parameters” area also allows the activation/deactivation of some elements by means of a check box that appears before its name (see 5.2.1). Consistency checks on the values inputted are done (from, to, <, numerical values...). The “to” zones can be left blank: in this case the parameter value is fixed. When the model calibration is executed, each active parameter will be initialized randomly using a value taken from the specified range. For compartments, the consistency check located after the zone “Minimal height” makes it possible to indicate whether the compartment has one. The corresponding input zone is active only if the box is checked. The representation of the compartment in the “Model” block is modified as a result.

The specific discharge coefficients k_{EM} , k_{EL} can be set proportional to k_{EC} .

5.2.5 Run parameters

This block is for inputting:

- different periods (warm-up, calibration, and validation). These periods cannot be overridden. For the warm-up period, the indication of beginning of period is the only one to be chosen. Warm-up and validation periods can be split up. In this case, the syntax is of the type: [beginning-end; beginning-end; ...]. The last indication can be designated by its numerical value or by “end”,
- the objective WOBJ function WOBJ, parametrizable via the adjoining button ,
- the threshold value $WOBJ_{min}$ (box grayed out in “run” mode),
- the number n_{obj} of simulations to conduct and requiring verification of the condition $WOBJ > WOBJ_{min}$ over the calibration period (box grayed out in “run” mode),
- the maximum execution time t_{max} beyond which the simulation is stopped, even if the number of simulations that have obtained an objective function value higher than the $WOBJ_{min}$ value remains less than n_{obj} (box grayed out in “run” mode),
- the folder in which the output files will be stored.

It also indicates the number of parameters to calibrate as a function of the chosen configuration and the ranges of values input for each parameter.

Remark The indexes begin at 0.

5.2.6 Calibration results

This block displays:

- the number of simulations that have reached an objective function value greater than the $WOBJ_{min}$ value for the calibration period,
- the value of the objective function over the calibration period,
- the value of the objective function for the validation period.

5.2.7 Command bar

The command bar is described in Table 1. Run mode allows the user to execute the model a single time using fixed parameter values:

- after execution in calibration mode, activation of run mode selects the value of parameters that have provided the optimal value of the objective criterion during the calibration period,
- parameter values can be modified by the user, making it possible to calibrate or conduct a manual sensitivity study,
- after loading a configuration (cm.properties file, see Section 5.3.2), execution in run mode makes it possible to recreate rainfall-discharge and rainfall and height graphs) corresponding to the simulation that has provided the optimal value of the objective criterion during the calibration period.






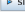
	Reset : sets all parameters to their default value
	Save : save the configuration (model structure, parameter values, simulation parameters) into a text file (CTRL+S) in the output directory specified in the “calibration results” area
	Open : opens a previously saved configuration (CTRL+O)
	Run : launches the model (CTRL+R) and: - shows the results (resulting parameters, objective function and graphics) - writes the output files
	CI : launches the Confidence Interval plot on the “P & Disch.” graph (block Results and Graphs)
	SI : calculates the Sobol Sensitivity Indexes and write the results in the “Sobol Sensit. Indexes” tab (block Results and Graphs)

Table 1: Command bar

5.2.8 Graphics

The value of the parameters in the set of optimal parameters, the values of performance measurements, and the various graphs produced by KarstMod are accessible via thumbnails in the general block “Results and graphs”. For all graphs a contextual menu can be accessed by a right click on the graph. This menu makes it possible to personalize the display parameters (type of scale: log or linear, fonts, colors...), make the toolbar appear or disappear, and make the different curves visible or invisible. The toolbar is presented in Table 2. It is possible to select a curve by clicking on it then moving the cursor with the direction arrows. The coordinates of a selected point are then displayed next to the toolbar.

Warning To optimize space, the toolbar is deactivated by default for some graphs. It can be reactivated via the contextual menu.

The following graphs are proposed/available:

- “P. & disch.”: Displays the P , ET , and pumped and observed discharge curves and the discharge curve corresponding to the set of optimal parameters selected as the outcome of the calibration. The various periods (warm-up, calibration, and validation) are represented by different background colors.
- “P. & internal disch.”: Displays the P and ET curves and the internal discharges of the model. The user can superimpose observed and calculated discharge curves (they are invisible by default).
- “P. & internal water levels”: Displays the P and ET curves and curves corresponding to water heights in the various compartments of the model, along with piezometric water levels (if available).
- “Cumulative volume”: Displays the cumulative curve of simulated and observed discharges for the calibration period. It also displays the “Volume error” ($\sum(Q_S - Q_{obs})/\sum Q_{obs}$) below. It provides two subgraphs (calibration & validation periods)
- “Mass balance”: per time step value of the model mass balance for the calibration and validation periods,
















	changes the color of the selected curve
	save curves values in a csv file
	separates the graphics from the main KarstMod windows
	multiplies zoom factor by 2 for the horizontal axis (default) or the vertical axis (⌘ key pressed)
	divides zoom factor by 2 for the horizontal axis (default) or the vertical axis (⌘ key pressed)
	adjusts vertical scale so that all curves are shown on the graph
	advanced configuration settings for the graphics
	prints the graphics
	exports the graphics as an image file
	sets the graph time scale to the limits of the warm-up period
	sets the graph time scale to the limits of the calibration period
	sets the graph time scale to the limits of the validation period
	sets the graph time scale to the limits of the warm-up, calibration and validation periods
	sets the spacing of time labels
	pop-up description of the graph

Table 2: Graph toolbar

- “ Q_S vs Q_{obs} ”: scatter plot of simulated vs observed discharge values
- “ $Q_S - Q_{obs}$ ”: discharge modelling error time series
- “Prob. plot”: probability plot for the observed and discharge time series. Provides two subgraphs (calibration & validation periods)
- “Corr P/Q ”: rainfall-discharge cross-correlogram for both observed and simulated discharge time series
- “Corr Q_{obs} / Q_S ”: observed vs simulated discharge cross-correlogram. Provides two subgraphs (calibration & validation periods)
- “Autocorr Q_{obs} & Q_S ”: auto-correlogram for both observed and simulated discharge time series. Provides two subgraphs (calibration & validation periods)
- “WOBJ vs param” scatter plots of the values of the objective function (calibration period) against the values of the parameters X_i , for all parameter sets of the Sobol sequence that satisfy $WOBJ > WOBJ_{min}$. These plots provide a preliminary analysis of the distribution of optimum values of each parameter. Also provides parameter values for the optimal parameter set (red dot).
- “OBJ1 vs OBJ2”: scatter plot of the values of the performance criteria used to define the aggregated objective function, for all parameter sets of the Sobol sequence that satisfy $WOBJ > WOBJ_{min}$. These plots make it possible to investigate potential conflicts between performance criteria (Pareto frontier) [6].
- “WOBJ cal vs val”: scatter plot of the calibration vs validation values of WOBJ
- “Sobol sensit. indexes”: variance-based, first-order S_i and total S_{T_i} sensitivity indexes for the model parameters X_i . These indexes help the user estimate the influence of parameters on model output, and thus to detect over-parameterization.

5.3 File format

5.3.1 Input data

The input data file contains the rainfall, evapotranspiration, pumped discharge and observed discharge and hydraulic head values. It is organized in 10 columns separated by tabs (See example in figure 4):

- column 1 - date (either yyyyMMdd or yyyyMMdd HH:mm format).
- column 2 - not used by the model.
- column 3 - rainfall P (mm/day for daily data, or mm/hour for hourly data),
- column 4 - evapotranspiration ET (mm/day for daily data, or mm/hour for hourly data),
- column 5 - discharge Q_{pump}^L pumped into compartment L (m^3/s),
- column 6 - discharge Q_{pump}^M pumped into compartment M (m^3/s),

- column 7 - discharge Q_{pump}^C pumped into compartment C (m^3/s),
- column 8 - discharge Q_{pump}^S pumped at the outlet (m^3/s),
- column 9 - discharge Q_{obs} observed at the outlet (m^3/s),
- column 10 - hydraulic head Z_{obs} measurements (m) (not mandatory).

Missing values of the observed discharge at the outlet can be replaced by the “INTERP” or “NOINTERP” value, depending on whether interpolation of the missing data is allowed (“INTERP”) or not (“NOINTERP”). Decimals can be separated by either points or commas. Exclamation marks are used for header lines.

```
! KARSTMOD INPUT FILE - EXAMPLE FOR VERSION 1.5
!
! date format must be either yyMMdd or yyyyMMdd HH:mm
! Missing values of the observed discharge at the outlet can be replaced by the "INTERP" or
! "NOINTERP" value, depending on whether interpolation of the missing data is allowed ("INTERP")
! or not ("NOINTERP"). Decimals can be separated by either points or commas. Exclamation marks are
! used for header lines.
!
!date      comment  P    ET    QpumpL  QpumpM  QpumpC  QpumpS  QobsS  Piezo
20000101 00:00  1-    0    0.4    0-    0-    0-    0-    0.76  0
20000102 00:00  2-    2.4  0.4    0-    0-    0-    0-    0.76  0
20000103 00:00  3-    8.7  0.4    0-    0-    0-    0-    0.76  0
20000104 00:00  4-    1    0.4    0-    0-    0-    0-    0.76  0
20000105 00:00  5-    0    0.4    0-    0-    0-    0-    0.76  0
20000106 00:00  6-    0    0.4    0-    0-    0-    0-    INTERP 0
20000107 00:00  7-    0    0.4    0-    0-    0-    0-    0.78  0
20000108 00:00  8-    7.9  0.4    0-    0-    0-    0-    0.77  0
20000109 00:00  9-    0    0.4    0-    0-    0-    0-    0.77  0
20000110 00:00  10-   1.4  0.4    0-    0-    0-    0-    INTERP 0
```

Figure 4: KarstMod input file example.

5.3.2 Output files

The KarstMod configuration (model structure, calibration parameters and optimal parameter set) can be saved and / or loaded in a configuration file (*.cm.properties).

After each run, three output files are generated automatically:

- params_best.csv contains the parameter set that yields the highest value of the objective function over the calibration period,
- discharge_out.csv contains the simulated discharge time series for the parameter set that yields the highest value of the objective function over the calibration period,
- params_out.csv contains all parameter sets that verify $WOBJ > WOBJ_{min}$ over the calibration period.

In run mode, the files are prefixed 'run'

Remark The water level of deactivated compartments and deactivated internal fluxes are arbitrarily set to zero.

Remark After loading a configuration (cm.properties file), execution of run mode makes it possible to recreate the rainfall-discharge and rainfall and height graphs that correspond to the simulation that provided the optimal value of the objective criterion during the calibration period.

6 Example

The Durzon spring is the outlet of a 115 km² area located South-East of France in the Larzac Causse. A 2-compartments global model of the rainfall-discharge relationship was proposed by Tritz et al. [18]. Calibration was performed on year 2003 using 2002 as a warm-up period and 2004-2008 for validation. Model performance was assessed using Nash-Sutcliffe efficiency and reaches 0.85 and 0.83 over the calibration and validation periods respectively.

KarstMod allows to successfully reproduce the model structure (see Fig. 5). The platform also allows a further analysis of the model functioning. Possible glimpses into model functioning are exemplified below using outputs from KarstMod version 1.5. For instance, the probability plot (Fig. 6) and the rainfall-discharge correlogram (Fig. 7) both confirm the good fit of the modelled and observed discharge distributions. However, the balance error is 17% over the calibration period, against only 7% over the validation period (KarstMod output). Keeping all parameters fixed to the optimal values proposed by [18], and calibrating the initial water levels leads to an unrealistic optimal value of the water level in the lower compartment (1800 mm - on peut mettre la figure 9), but to a better (5%) water balance on both the calibration and validation periods. The drift in the internal water levels thus compensates an inadequate model input: the model “lacks” some water. Calibration of both the initial water levels and the recharge area leads to realistic values of the initial water levels and a recharge area of 140 km², with a low balance error on the calibration period but with a 17% balance error on the validation period. This difficulty to satisfy the water balance in both calibration and validation period indicates that further work on the meteorological inputs may be required.

Now, let's consider the hysteretic discharge function Q_{hy} from compartment E to compartment C :

$$Q_{hy} = \varepsilon_{HY} \times k_{hy} \left(\frac{E - E_{hy}}{L_{ref}} \right)^{\alpha_{hy}} \quad (14)$$

where k_{hy} is the specific discharge coefficient [L/T], α_{hy} is a positive exponent [-], and ε_{hy} [-] is an indicator of the activation of the hysteretic discharge. ε_{hy} is switched to 1 if E rises above $E_{hy} + \Delta E_{hy}$ and it is switched to 0 if E falls below E_{hy} . This discharge function is defined by 4 parameters, and the authors placed much emphasis on the hysteretic activation. The per-time-step simulated against measured discharge graph (Fig 10.a) shows that the model tends to underestimate peak flows. Automatic calibration using KarstMod (Fig 10.b) yields slightly better results. We realised an automatic calibration of two modified models: (i) ε_{HY} equal to 1 (no hysteretic activation), (ii) α_{hy} equal to 1 (linear transfer function). The de-activation of the hysteretic transfer yields slightly under-estimated medium flows values (Fig. 10.c). The de-activation of the α_{hy} coefficient has a heavy impact on the high-flows simulation (Fig. 10.d). The key variable for high flow simulation in the proposed hysteretic discharge function thus seems to be the α_{hy} exponent, whereas medium flows are dependent on the hysteretic activation of the transfer.

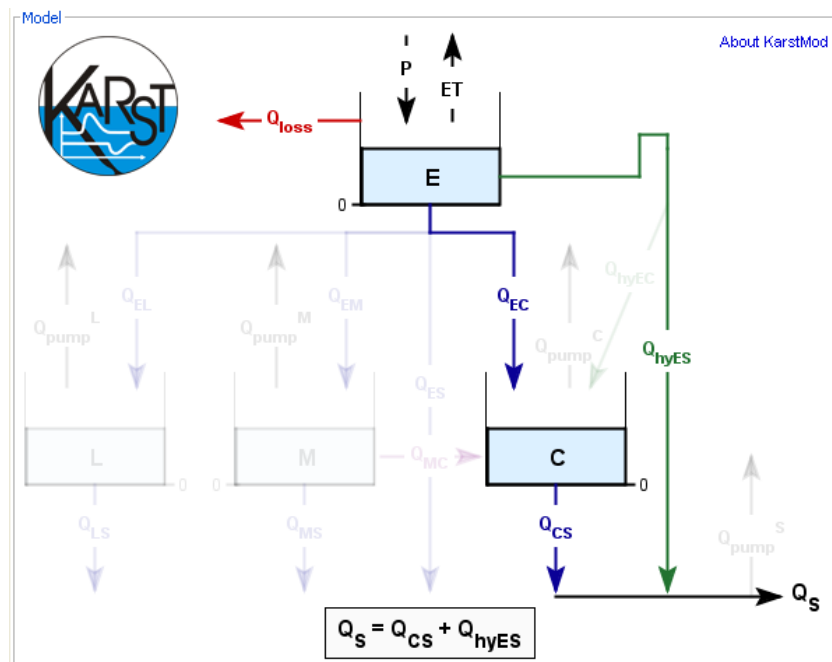


Figure 5: Model structure for the Durzon karst system. Unselected compartments and fluxes are grayed out.

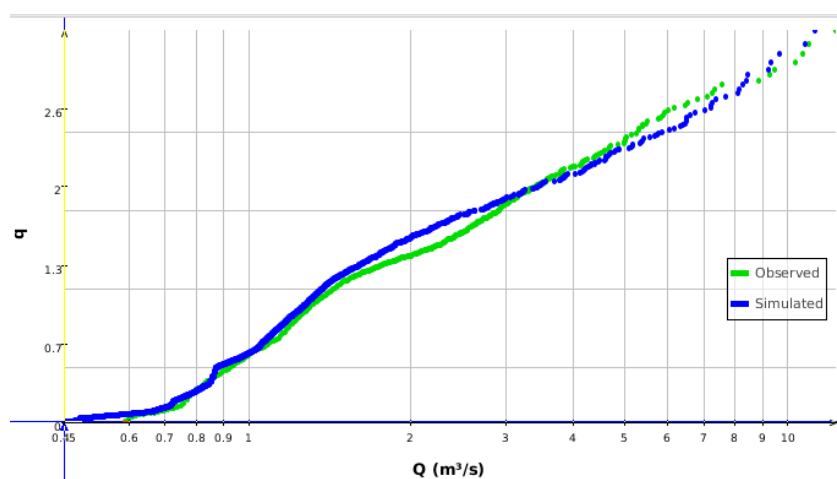


Figure 6: Probability plot for the Durzon model.

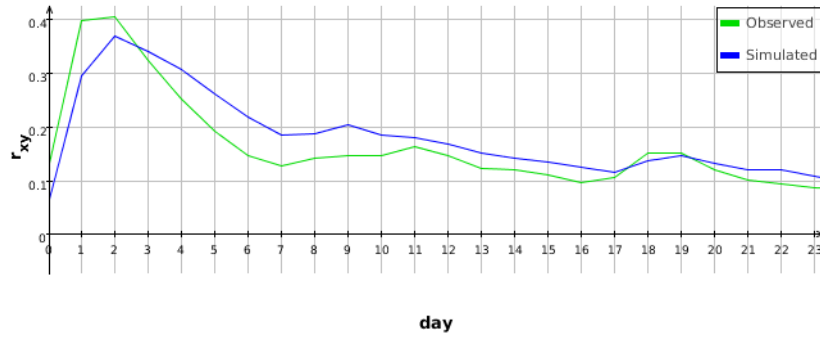


Figure 7: Rainfall-discharge correlogram for the Durzon model.

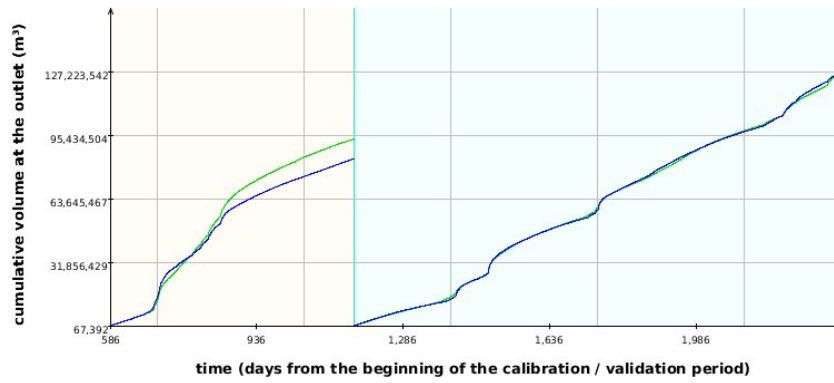


Figure 8: Cumulative volume at the outlet of the Durzon model.

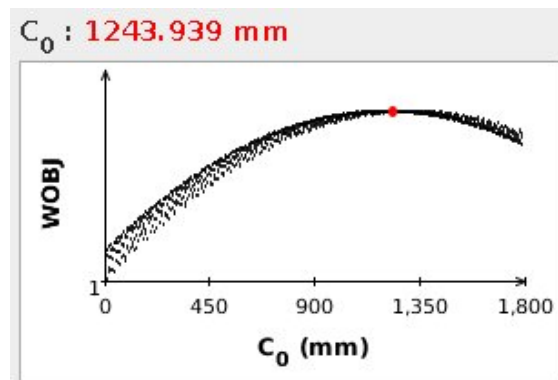


Figure 9: Durzon model: Nash-Sutcliffe efficiency over the calibration period as a function of the initial water level C_0 in compartment C.

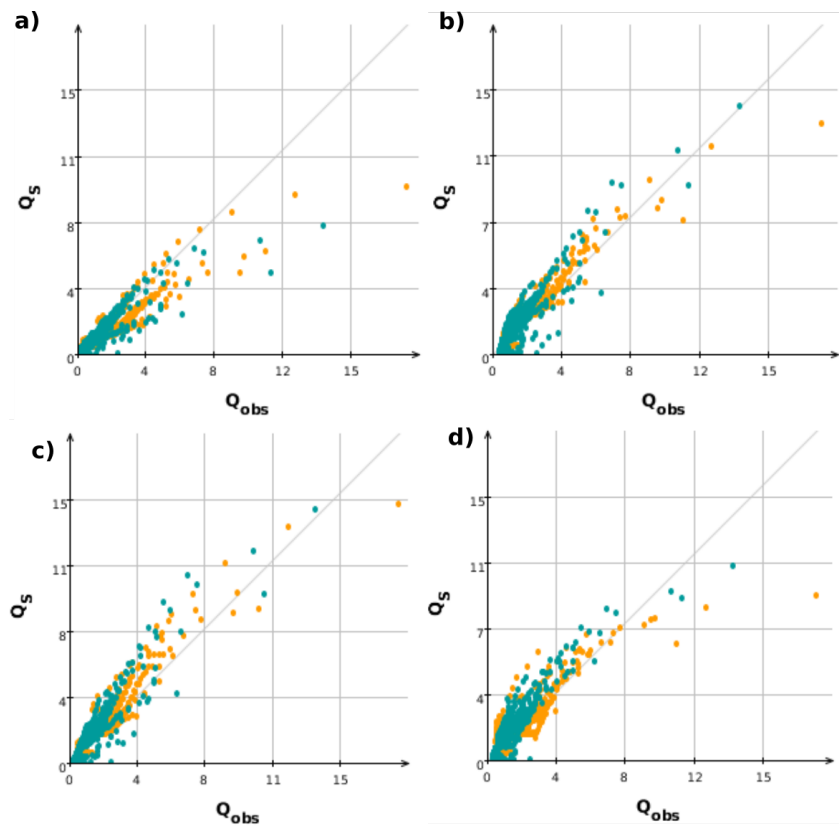


Figure 10: Measured against simulated discharge for the Durzon model for: a) the parameter set proposed by [18], b) the optimal KarstMod solution, c) the modified Durzon model with no hysteretic activation of the upper compartment to spring transfer function, d) the modified Durzon model with no exponent coefficient in the hysteretic function.

A Model solution

A.1 Analytical solutions (linear cases)

In compartments where all exponents are set equal to 1, we use the analytical solution of the differential model equations. These analytical solutions are detailed below for the cases when inter-compartment coupling is considered (Section A.1.2) or not (Section A.1.1). Note that practical implementation of the analytical solutions in KarstMod takes into account discharge laws activation and deactivation due to threshold crossing within a model time step.

A.1.1 Analytical solution - Linear rainfall-discharge case with no inter-compartment coupling

We consider the following mass balance equation for compartment A:

$$\frac{dA(t)}{dt} = S(t) - \sum_{i=1}^n k_i(A(t) - A_{s_i}) = S - \sum_{i=1}^n Q_i(t) \quad (15)$$

where S is a source term (e.g. $P-ET$ for compartment E, or $Q_{EL} - Q_{pumpL}$ for compartment L), k_i is the specific discharge coefficient for discharge law i (e.g. k_{EC} , k_{EL} , k_{loss} , ...) and A_{s_i} is the activation level for discharge law i (e.g. E_{hy} , E_{loss} , or 0). Equation 15 may be rewritten as follows

$$\frac{dA(t)}{dt} = S' - kA(t) \quad (16)$$

with $S' = S + \sum_{i=1}^n k_i A_{s_i}$ and $k = \sum_{i=1}^n k_i$. The analytical solution of 16 is

$$A(t) = \frac{S'}{k} + \left(A_0 - \frac{S'}{k} \right) \exp(-kt) \quad (17)$$

Between time step n and time step $n + 1$ (time-stepping Δt), the source term $S(t)$ is constant. Thus,

$$A_{n+1} = \frac{S'_n}{k} + \left(A_n - \frac{S'_n}{k} \right) \exp(-k\Delta t) \quad (18)$$

The average outflow from compartment A between n and $n + 1$ is

$$Q_n = S'_n + \frac{A_n - A_{n+1}}{\Delta t} \quad (19)$$

and

$$Q_{i,n} = \frac{k_i A_n}{k} Q_n - k_i A_{s_i} \quad (20)$$

A.1.2 Analytical solution for rainfall-discharge relationship with inter-compartment coupling

We consider the following mass balance equation for compartments M and C:

$$\frac{dM}{dt} = k_{MC}(C - M) - k_{MS}M + S_M \quad (21a)$$

$$\frac{dC}{dt} = k_{MC}(M - C) - k_{CS}C + S_C \quad (21b)$$

where S_M , S_C are the source terms:

$$S_M = Q_{EM} - Q_{pumpM} \quad (22a)$$

$$S_C = Q_{EC} - Q_{pumpC} \quad (22b)$$

Case $k_{MS} = k_{CS} = 0$ Combining equations 21 brings:

$$\frac{d(M + C)}{dt} = S_M + S_C \quad (23a)$$

$$\frac{d(M - C)}{dt} = -2k_{MC}(M - C) + S_M - S_C \quad (23b)$$

Assuming S_M and S_C constant,

$$M(t) + C(t) = (S_M + S_C)t + M_0 + C_0 \quad (24a)$$

$$M(t) - C(t) = \frac{S_M - S_C}{2k_{MC}} + \left(M_0 - C_0 - \frac{S_M - S_C}{2k_{MC}} \right) \exp(-2k_{MC}t) \quad (24b)$$

The combination of equations 24 brings

$$M(t) = \frac{M_0 + C_0}{2} + \frac{S_M + S_C}{2}t + \frac{S_M - S_C}{4k_{MC}} + \frac{1}{2} \left(M_0 - C_0 - \frac{S_M - S_C}{2k_{MC}} \right) \exp(-2k_{MC}t) \quad (25a)$$

$$C(t) = \frac{M_0 + C_0}{2} + \frac{S_M + S_C}{2}t - \frac{S_M - S_C}{4k_{MC}} - \frac{1}{2} \left(M_0 - C_0 - \frac{S_M - S_C}{2k_{MC}} \right) \exp(-2k_{MC}t) \quad (25b)$$

Between time step n and time step $n + 1$ (time-stepping Δt):

$$M_{n+1} = \frac{M_n + C_n}{2} + \frac{S_M + S_C}{2}\Delta t + \frac{S_M - S_C}{4k_{MC}} + \frac{1}{2} \left(M_n - C_n - \frac{S_M - S_C}{2k_{MC}} \right) \exp(-2k_{MC}\Delta t) \quad (26a)$$

$$C_{n+1} = \frac{M_n + C_n}{2} + \frac{S_M + S_C}{2}\Delta t - \frac{S_M - S_C}{4k_{MC}} - \frac{1}{2} \left(M_n - C_n - \frac{S_M - S_C}{2k_{MC}} \right) \exp(-2k_{MC}\Delta t) \quad (26b)$$

Other cases Equation (21) may be rewritten into

$$d_t \mathbf{v} = \mathbf{A} \mathbf{v} + \mathbf{s}, \quad \mathbf{A} = \begin{bmatrix} -k_{MC} - k_{MS} & k_{MC} \\ k_{MC} & -k_{MC} - k_{CS} \end{bmatrix}, \quad \mathbf{v} = \begin{bmatrix} M \\ C \end{bmatrix}, \quad \mathbf{s} = \begin{bmatrix} S_M \\ S_C \end{bmatrix} \quad (27)$$

The eigenvector formulation for 27 is

$$d_t \mathbf{w} = \Lambda \mathbf{w} + \mathbf{s}' \quad (28)$$

with $\Lambda = \text{diag}(\lambda_1, \lambda_2)$, $\mathbf{s}' = \mathbf{K}^{-1} \mathbf{s}$ et $\mathbf{w} = \mathbf{K}^{-1} \mathbf{v}$. Equation 28 can be rewritten as

$$d_t w_p = \lambda_p w_p + s'_p, \quad p = 1, 2 \quad (29)$$

The analytical solution of 29 is

$$w_p(t) = w_p^{\text{eq}} + (w_p(0) - w_p^{\text{eq}}) \exp(-\lambda_p t), \quad p = 1, 2 \quad (30a)$$

$$w_p^{\text{eq}} = \frac{s'_p}{\lambda_p} \quad (30b)$$

In our case

$$\lambda_1 = - \left(k_{MC} + \frac{k_{MS} + k_{CS}}{2} \right) - \left[\left(k_{MC} + \frac{k_{MS} + k_{CS}}{2} \right)^2 - (k_{MS}k_{MC} + k_{CS}k_{MC} + k_{MS}k_{CS}) \right]^{1/2} \quad (31)$$

$$\lambda_2 = - \left(k_{MC} + \frac{k_{MS} + k_{CS}}{2} \right) + \left[\left(k_{MC} + \frac{k_{MS} + k_{CS}}{2} \right)^2 - (k_{MS}k_{MC} + k_{CS}k_{MC} + k_{MS}k_{CS}) \right]^{1/2} \quad (32)$$

and

$$\mathbf{K} = \begin{bmatrix} k_{MC} & \lambda_2 + k_{MC} + k_{CS} \\ \lambda_1 + k_{MC} + k_{MS} & k_{MC} \end{bmatrix} \quad (33)$$

Hence,

$$\mathbf{K}^{-1} = \frac{1}{\det \mathbf{K}} \begin{bmatrix} k_{MC} & -\lambda_2 - k_{MC} - k_{CS} \\ -\lambda_1 - k_{MC} - k_{MS} & k_{MC} \end{bmatrix} \quad (34)$$

with

$$\det \mathbf{K} = k_{MC}^2 - (\lambda_1 + k_{MC} + k_{MS})(\lambda_2 + k_{MC} + k_{CS}) \quad (35)$$

The state variables are obtained from $\mathbf{v}(t) = \mathbf{K} \mathbf{w}(t)$.

Outflow The total outflow from compartments M and C between time steps n and $n + 1$ is

$$Q_{MS,n} + Q_{CS,n} = \frac{M[n] - M[n+1]}{\Delta t} + \frac{C[n] - C[n+1]}{\Delta t} + S_{M,n} + S_{C,n} \quad (36)$$

Note that S_M, S_C are constant over the time step. The outflows from compartments M and C towards the spring and the inter-compartment flow are provided by

$$Q_{MS} = (Q_{MS} + Q_{CS}) \times \frac{k_{MS} \times M_{n,n+1}}{k_{MS} \times M_{n,n+1} + k_{CS} \times C_{n,n+1}} \quad (37a)$$

$$Q_{CS} = (Q_{MS} + Q_{CS}) \times \frac{k_{CS} \times C_{n,n+1}}{k_{MS} \times M_{n,n+1} + k_{CS} \times C_{n,n+1}} \quad (37b)$$

$$Q_{MC} = \frac{M_n - M_{n+1}}{\Delta t} + S_M - Q_{MS} \quad (37c)$$

where

$$M_{n,n+1} = \frac{M_n + M_{n+1}}{2} \quad (38a)$$

$$C_{n,n+1} = \frac{C_n + C_{n+1}}{2} \quad (38b)$$

A.2 Linearized formulations

Non-linear formulations are solved using a second-order Runge-Kutta scheme of the linearized formulation.

Discharge-water level functions Q_{AB} , Q_{loss} , Q_{hy} with non-unitary exponent of the form $Q(t) = k(A(t) - A_s)^\alpha$ are approximated into

$$Q(t) = k'_n(A(t) - A_s) \quad (39a)$$

$$k'_n = k(A_n - A_s)^{(\alpha-1)} \quad (39b)$$

Inter-compartment discharge function of the form $Q = k \operatorname{sgn}(M - C) |M - C|^{\alpha_{MC}}$ is approximated into

$$Q = k'_n(M - C) \quad (40a)$$

$$k'_n = k |M_n - C_n|^{\alpha_{MC}-1} \quad (40b)$$

List of Notations

$\overline{Q_{obs}}$	mean value of Q_{obs} (L^3/T)
α_{AB}	general notation for the positive exponent of the discharge-water level function from compartment A to compartment B (assumed to be positive)
α_A	exponent for the infinite time scale transfer function for compartment A $\alpha^A \in]0, 1[$ (-)
α_{loss}	positive exponent for the threshold loss function (-)
ΔE_{hy}	threshold for the activation of the Q_{hy} function (L)
τ_A	time scale for the infinite time scale transfer function for compartment A (T)
ε_{hy}	binary indicator of the activation of the hysteretic discharge
A, B	general notation for the water level in compartment A, B (L)
E_{hy}	threshold for the deactivation of the Q_{hy} function (L)
E_{loss}	threshold for the activation of the Q_{loss} function (L)
E_{min}	minimum water level in compartment E (L)
ET	evapotranspiration rate (L/T)
$h_{max A}$	upper threshold for the water levels in sub-compartments of a compartment with infinite characteristic time scale configuration (L)
$h_{min E}$	lower threshold for the water levels in sub-compartments of compartment E (infinite characteristic time scale configuration) (L)
k_{AB}	specific discharge coefficient for linear discharge law from compartment A to compartment B (L/T)
k_{hy}	specific discharge coefficient for the hysteretic discharge (L/T)
k_{loss}	specific discharge coefficient for the Q_{loss} function (L/T)
L_{ref}	reference length for normalisation of the water level of compartment A
n_{obj}	target number of simulations to achieve $WOBJ > WOBJ_{min}$
P	precipitation rate (L/T)
Q_{AB}	general notation for the discharge from compartment A to compartment B per unit surface area (L/T)
Q_{bA}	general notation for the base discharge from compartment A with infinite characteristic time scale configuration, per unit surface area (L/T)
Q_{hyEC}	hysteretic discharge from compartment E to compartment C per unit surface area (L/T)
Q_{hyES}	hysteretic discharge from compartment E to the outlet S per unit surface area (L/T)
Q_{hy}	total hysteretic discharge from compartment E per unit surface area (L/T)
Q_{loss}	discharge lost from compartment E per unit surface area (L/T)
Q_{obs}	observed discharge (L^3/T)
Q_{pump}^A	discharge rate abstracted from compartment A per unit surface area (L/T)
Q_{rA}	general notation for the overflow discharge from compartment A with infinite characteristic time scale configuration, per unit surface area (L/T)
Q_S	discharge at the outlet (L^3/T)
R_A	recharge area (L^2)
sgn	signum function
t_{max}	maximum simulation duration (T)
w	coefficient $\in [0, 1]$ used for weighting the performance criteria (-)
x_{EC}	distribution coefficient for Q_E towards the E and C compartments (-)

x_{EM}	distribution coefficient for Q_E towards the E and M compartments (-)
x_{hy}	distribution coefficient for Q_{hy} towards compartment C and the spring (-)
A, B	general notation for the compartments: either E, L, M, C, and the outlet: S
BE	balance error (-)
KGE	Kling-Gupta Efficiency (-)
NSE	Nash-Sutcliffe efficiency model performance criteria (-)
VE	volume error (-)
WOBJ	objective function
$WOBJ_{min}$	threshold value of the objective function

References

- [1] Beven K. & Binley A. 1992. The future of distributed models: Model calibration and uncertainty prediction. *Hydrological Processes*, John Wiley & Sons Ltd, 6, 279-298
- [2] Beven K. 2006. A manifesto for the equifinality thesis. *Journal of Hydrology*, 320, 18-36
- [3] Ebel B. A. & Loague K. 2006. Physics-based hydrologic-response simulation: Seeing through the fog of equifinality. *Hydrological Processes*, 20, 2887-2900
- [4] Guinot V., Cappelaere B., Delenne C. & Ruelland D. 2011. Objective functions for conceptual hydrological model calibration: Theoretical analysis of distance and weak form-based functions. *Journal of Hydrology*. 401(1-13)
- [5] Guinot, V., Savéan, M., Jourde, H., and Neppel, L. 2015. Conceptual rainfall-runoff model with a twoparameter, infinite characteristic time transfer function. *Hydrol. Process.*, 29: 4756-4778
- [6] Gupta H. V., Sorooshian S. & Yapo P. O. 1998. Toward improved calibration of hydrologic models: Multiple and noncommensurable measures of information. *Water Resources Research*, 34, 751-763
- [7] Gupta, Hoshin V., Harald Kling, Koray K. Yilmaz Guillermo F. & Martinez. 2009. Decomposition of the mean squared error and NSE performance criteria: Implications for improving hydrological modelling. *Journal of Hydrology*, 377(1-2), pp 80-91. doiI: 10.1016/j.jhydrol.2009.08.003.
- [8] Hogue T.S., Gupta H., Sorooshian S. 2006. A 'User-Friendly' approach to parameter estimation in hydrologic models. *Journal of Hydrology* 320, 207-217.
- [9] Hornberger G. & Spear R. 1981. An approach to the preliminary analysis of environmental systems. *Journal of Environmental Management*, 12, 7-18
- [10] Mangin A. 1975. [Contribution à l'étude hydrodynamique des aquifères karstique. PhD thesis, University of Dijon \(France\)](#)
- [11] Marsaud B., 1996. Structure et fonctionnement de la zone noyée des karsts à partir des résultats expérimentaux. Thèse de doctorat Orsay, Université Paris XI.
- [12] Moussa R., 2010. When monstrosity can be beautiful while normality can be ugly: assessing the performance of event-based flood models. *Hydrological Sciences Journal*, 55(6), 1074-1084, doi:10.1080/02626667.2010.505893
- [13] Nash J.E. & Sutcliffe J., 1970. River flow forecasting through conceptual models : Part 1. A discussion of principles. *J. Hydrol.* 10 (3), 282-290.
- [14] Perrin C., Michel C. & Andreassian V. 2001. Does a large number of parameters enhance model performance ? Comparative assessment of common catchment model structures on 429 catchments. *J. Hydrol.* 242(3-4), 275-301.
- [15] Saltelli A., Ratto, M., Andres T., Campolongo F., Cariboni J., Gatelli D., Saisana M. & Tarantola S. 2008. *Global Sensitivity Analysis. The Primer*, John Wiley & Sons.
- [16] Saltelli A. 2002. Making best use of model evaluations to compute sensitivity indexes. *Computer Physics Communications* 145, 280-297.
- [17] Sobol I., 1977. Uniformly Distributed Sequences with an Additional Uniform Property. *USSR Computational Mathematics and Mathematical Physics*, 16, 236-242.
- [18] Tritz S., Guinot, V. & Jourde, H. 2011. Modelling the behaviour of a karst system catchment using non linear hysteretic conceptual. model *Journal of Hydrology*, 397, 250-262, doi:10.1016/j.jhydrol.2010.12.001